TECHNICAL MEMORANDUMS

NATIONAL ADVISORY COMMITTEE FOR AERONAUTICS

No. 787

INVESTIGATIONS ON THE AMOUNT OF DOWNWASH BEHIND

RECTANGULAR AND ELLIPTICAL WINGS

By H. Muttray

Washington
February 1936

NATIONAL ADVISORY COMMITTEE FOR AERONAUTICS

TECHNICAL MEMORANDUM NO. 787

INVESTIGATIONS ON THE AMOUNT OF DOWNWASH BEHIND

RECTANGULAR AND ELLIPTICAL WINGS*

By H. Muttray

SUMMARY

The downwash behind a wing may be computed from the system of vortices created by the wing and which can be substituted for the latter. If the actual rolling-up process of the free vortex sheet is disregarded hereby, the establishment of boundaries for the downwash factors is contingent upon the premise that no rolling up takes place or else that the developed tip vortices start direct on the effective line. The actual downwash factors for the rectangular wing are rather of the approximate magnitude of the values computable with the developed tip vortices starting direct on the wing. Hereby we encounter a relationship with the c_a value: the downwash factors referred to the induced angle of attack become smaller as c_a increases.

The latter is even more true for the elliptical wing. On it the downwash factors already reach at low angles of attack the amount of those given through the nonrolled vortex sheet, provided the distance downstream from the wing does not exceed 1.5 times the semispan.

The survey of the position of the tip-vortex cores on the elliptical wing reveals that the cores do not reach the theoretical value save at very great distance. (The present report treats the wing alone, i.e., without consideration of body or slipstream effects, although downwash experiments on "wings with fuselage" and "wings with fuselage and rotating propeller" are under way.)

I. INTRODUCTION

The direction of the air stream at any point behind the wing can be computed from the vortex system, for which the wing may be replaced and which the latter creates – "bound" and "free" vortices.

For predetermined spanwise lift or circulation distribution $\Gamma = f(x)$, the strength of the free vortex shedding between x and dx and extending to infinity, is

$$d\Gamma = \frac{\partial \Gamma}{\partial x} dx \tag{1}$$

The field of flow behind the wing, visualized thereby as effective line, is thus characterized by an infinite number of individual trailing vortices with a common line of symmetry and a common bound vortex axis.

Every single vortex of the system is then affected by the other vortices, with the result that the thus-formed vortex sheet is not in flow direction but rather slightly lowered. However, this amount is so small as to be negligible, as a rule.

This lowering of the vortex sheet may be so much more negligible as, apart from that, another rolling-up process of the vortex sheet (reference 1), not exactly known in its individual phases, shifts the picture considerably, for the vortex sheet is unstable. It rolls up into two distinct tip vortices almost directly behind the wing (reference 2) and so creates a vortex distribution as shown in figure 1. With predetermined lift distribution $\Gamma = f(x)$ over the span b, the distance b' of the expressed tip vortices can be readily computed (references 2, 3, 4) by means of the momentum theorem for the steady flow. It affords the relation:

$$b' = \frac{1}{\Gamma_m} \int_{-b/2}^{+b/2} \Gamma \, dx \tag{2}$$

(Γ_m = circulation in wing center).

The sum of the circulations of the free vortices of a semiwing equals, according to (1), the circulation at wing center. No circulation being lost (reference 5) during the rolling-up process of the vortex sheet, the circulation of the developed individual tip vortices likewise equals Γ_m.

Now when it is assumed that these developed separate tip vortices start directly on the effective line, substituting for the wing, rather than at some distance behind the wing after the rolling-up process of the vortex sheet is completed, then the so-called "bound" vortices must likewise be replaced by one single vortex of strength Γ_m. In this manner we arrive at the initially cited replacement of the theoretical vortex system by one single horseshoe or trailing vortex.

The calculation of the downwash itself is then fairly simple and yields, as shall be shown, values which are fairly in accord with the experimental figures. The values are lower than those obtained with nonrolled vortex sheet. The figures for the latter represent an upper limit. A lower limit is obtained by assuming the circulation to be uniformly distributed over the total span (references 3 and 6). The vortex strength is then $\overline{\Gamma}$.

In the particular case of a simple trailing vortex with circulation Γ and the free vortex spacing a, the application of the Biot-Savart theorem gives for a point on the line of symmetry of the vortex arrangement, the following term for the inference velocity w at right angles to the plane in which the vortices lie:

$$w = \frac{\Gamma}{\pi a} \left(1 + \frac{\sqrt{l^2 + \left(\frac{a}{2}\right)^2}}{l} \right)$$

(l = distance of point in flow direction from the bound vortex.)

Putting a = b ("lower limit") and the angle of downwash at

$$\alpha_w = \frac{w}{v}$$

where v = undisturbed velocity, we have:

$$\alpha_w = \frac{\overline{\Gamma}}{\pi \, b \, v} \left(1 + \frac{\sqrt{l^2 + \left(\frac{b}{2}\right)^2}}{l} \right)$$

with

$$\overline{\Gamma} = c_a \frac{Fv}{2b}, \quad \alpha_i = \frac{c_a}{\pi} \frac{F}{b^2} \quad \text{and} \quad \epsilon_l = \frac{l}{b/2}$$

wherein F = wing area and

α_i = induced angle of attack for elliptical lift distribution, it is

$$\frac{\alpha_W}{\alpha_i} = \frac{1}{2}\left(1 + \sqrt{1 + \frac{1}{\epsilon_l^2}}\right) \tag{3}$$

which, evaluated, gives:

$$\epsilon_l = \quad \frac{1}{3} \qquad \frac{2}{3} \qquad 1 \qquad 2$$

$$\frac{\alpha_W}{\alpha_i} = \; 2.08 \quad 1.4 \quad 1.21 \quad 1.06$$

It is seen that at great distance behind the wing the lower-limit value of the angle of downwash approaches asymptotically the value of the angle of downwash at the point of a wing with elliptical lift distribution.

For a wing with elliptical lift distribution and non-rolled vortex sheet ("upper limit"), the downwash factors of the line of symmetry afford an integral term (references 3 and 6) which, evaluated in tabulated form, is:

$$\epsilon_l = \quad \frac{1}{3} \qquad \frac{2}{3} \qquad 1 \qquad 2$$

$$\frac{\alpha_W}{\alpha_i} = \; 3.23 \quad 2.43 \quad 2.22 \quad 2.06$$

It is seen that the upper-limit value of the angle of downwash approaches, at great distance behind the wing, the double amount of the value at the point of the wing asymptotically. With

$$\frac{b'}{b} = \frac{F}{F_m} = k \tag{4}$$

$$\frac{\alpha_W}{\alpha_i} = \frac{1}{2}\frac{1}{k^2}\left(1 + \sqrt{1 + \frac{k^2}{\epsilon_l^2}}\right) \tag{3'}$$

for the wing with expressed single-tip vortices of spacing b'. The α_W/α_i values are shown plotted in figure 2 for different k values versus ϵ_l, according to (3').

This merely leaves the determination of the particular k for a given wing.

For a wing with elliptical lift distribution

$$\Gamma = \Gamma_m \sqrt{1 + \left(\frac{x}{b/2}\right)^2}$$

in conjunction with (2) gives:

$$k_{ell} = \frac{\pi}{4} = 0.785$$

For wings with rectangular lift distribution and constant profile and angle of attack, the k value is dependent on the aspect ratio $\lambda = b/t$ divided by the light gradient

$$n = \frac{dc_a}{d\ \alpha}$$

because the lift distribution itself is dependent on k.

Betz, in his thesis "Contribution to Airfoil Theory with Special Reference to the Simple Rectangular Wing" (reference 7), gives k in terms of L:

$$L = \frac{b}{t}\ \frac{4}{d\ c_a/d\alpha}\ \frac{A}{A_\infty} = \lambda\ \frac{4}{d\ c_a/\cdot d\alpha_\infty} \tag{5}$$

($d\ c_a/d\alpha$ = lift gradient of wing of finite aspect ratio; $d\ c_a/d\alpha_\infty$ = lift gradient for infinite aspect ratio.)

Putting

$$\frac{dc_a}{d\alpha_\infty} = 2\pi$$

that is, equal to the theoretical lift gradient for flat plates of infinite length, the pertinent aspect ratio is:

$$\lambda = \frac{b}{t} = \frac{\pi}{2} L \tag{6}$$

Glauert (reference 6) and Helmbold (reference 3) extrapolated Betz's k value in function of L, according to (6) for different λ. This approach may, however, be fore-

gone, because Betz gives L for rectangular lift distri-
bution also in function of $\frac{b}{t} \frac{1}{dc_a/d\alpha}$. Accordingly, we
show k in figure 3 in function of L, $\frac{b}{t}$ (whereby $\frac{dc_a}{d\alpha_\infty}$ =
2π!) and $\frac{b}{t} \frac{1}{dc_a/d\alpha}$.

II. EXPERIMENT

1. Experimental Procedure

The angle of downwash was measured with a so-called
"two-finger" downwash recorder (reference 8), with an in-
strumental accuracy of around $\pm 0.1^\circ$. Two superimposed
pitot tubes set at about 90° to each other were connected
through an inclined tube manometer. The tube assembly was
turned until the manometer indicated zero pressure differ-
ence; thus the angle of downwash could be read direct on a
scale. Of course, it was first necessary to establish the
sum of the setting angles between the aerodynamic zero di-
rection of the tube assembly and the pointer as well as
the scale zero through a special test (reference 9). The
instrument was mounted on a sliding support in the wind
shadow, which permitted pointing at any place behind the
wing. The test was made in the 2.25 m (7.38 ft.) wind tun-
nel of the AVA at Göttingen. The air speed was v = 30
m/s (98.4 ft./sec.). Altogether we measured three wings:

1. Rectangular, airfoil No. 387,
    t = 20 cm (7.87 in.), $\lambda = 5$

2. Rectangular, airfoil No. 422,
    t = 20 cm (7.87 in.), $\lambda = 5$

3. Elliptical, airfoil No. 387,
    t_{max} = 25.55 cm (10 in.), $\lambda = 5$,
    same area as rectangular wings.

We recorded the angle of downwash behind the wing on
more or less numerous axes (longitudinal, lateral, and
normal), at different angles of attack and, in addition,
the position of the tip vortex cores for profile No. 1.
We also measured the wing polars for the elliptical pro-
file with and without turbulence grid. The downwash meas-
urements, having been made in stages extending over a great

period of time, were, upon completion, followed by a check test on the symmetry longitudinal axis at height of the c.p. of the wing with increasing angle of attack, which afforded a quick cross section of the previously made measurements. The agreement with the previous measurements was satisfactory.

2. Evaluation

Aside from the previously mentioned constant correction involved with the use of the downwash recorder, another correction had to be effected on the read angle of downwash which was bound up with the finite limitation of the experimental jet diameter.

The jet diameter being finite, the wing causes – as is known – a deflection of the total air stream, which at the point of the wing is half as much as it is far behind the wing. The amount of deflection at the point of the wing and at points far behind the wing can be computed when assuming reflected free vortices to both sides of the jet. This does not require the substitution of the vortex sheet for the wing. When the wing span is less than three-fourths of the jet diameter, it suffices to proceed from constant spanwise lift distribution (reference 6).

In this case the Biot-Savart theorem applied to the reflected vortex gives the angle of downwash correction at the point of wing center at:

$$\varphi_o = \frac{c_a}{8} \frac{F}{F_o}$$

(F = wing area, F_o = jet section). Contrariwise, proceeding from elliptical lift distribution, we obtain, for, instance, for the conditions in the 2.25 m (7.38 ft.) Gottingen wind tunnel ($F = 0.2$ m² (2.15 sq.ft.), $b = 1.0$ m (3.28 ft.) jet diameter $R = 1.125$ m (3.69 ft.), the value

$$\varphi_{o_{ell}} = \frac{c_a}{8} \frac{F}{F_o} 1.009^*$$

that is, not quite 1-percent difference.

The term for the angle of downwash correction on the

*I. Lieferung d. Ergebnisse d. AVA zu Göttingen.

jet axis as function of the spacing factor $\epsilon_l = \dfrac{l}{b/2}$ is obtained in the same way for rectangular distribution over the total span at approximately:

$$\varphi = \varphi_0 \left(1 + \frac{\epsilon_l}{\sqrt{\epsilon_l{}^2 + m^4}} \right) \tag{7}$$

where $m = \dfrac{R}{b/2}$.* An exact theory is lacking up to the present. Referred to the induced angle of attack α_i for elliptical lift distribution, we have.

$$\frac{\varphi}{\alpha_i} = \frac{1}{2m^2} \left(1 + \frac{\epsilon_l}{\sqrt{\epsilon_l{}^2 + m^4}} \right) \tag{8}$$

Lastly, proceeding from a constant lift distribution over span $b' = k\,b$ rather than over the total span, affords

$$\frac{\varphi'}{\alpha_i} = \frac{1}{2m^2} \left(1 + \frac{\epsilon_l}{\sqrt{\epsilon_l{}^2 + \frac{m^4}{k^2}}} \right) \tag{9}$$

The difference between (8) and (9) being so insignificant, we simply used (7) and (8) for angle of downwash corrections.

3. Test Results

a) Rectangular wing, airfoil No. 387.- The results of the aerodynamic force measurements are shown in figures 4 and 5, the latter also including the values of $dc_a/d\alpha$ in radians.

The angle of downwash was recorded at $\alpha = -3.1°$, $-0.2°$, $+4.2°$, $+8.6°$, $+12.5°$, and $+14.0°$ on more or less numerous longitudinal, lateral, and normal axes. Figures 6 to 8 are examples of records taken at $\alpha = 8.6°$ and $c_a = 1.065$. The distribution of the downwash factors α_w^a/α_i on the individual axes being similar at all α, it

*Miss I. Lotz has, in the interim, established an accurate theory for this. On the other hand, the experimental figures given in the present report vary within negligibly narrow limits, when the exact theoretical correction factors are applied.

seemed unnecessary to publish all the test results aside from $\alpha = 8.6^\circ$, except the values of the longitudinal axes through the origin of the chosen system of coordinates (fig. 9). These values are, in part, direct measurements; in part, interpolations.

The notation used in the graphs are:

l is the distance of test station from bound vortex, downstream, in direction of longitudinal axis

q,   distance of test station from plane of symmetry of wing in lateral axis direction (+ q = starboard wing)

h,   distance of test station in direction of normal axis (+ h = suction side, - h = pressure side)

$$\epsilon_l = \frac{l}{b/2} \; , \quad \epsilon_q = \frac{q}{b/2}, \quad \epsilon_h = \frac{h}{b/2} = \text{spacing factors}$$

$$\frac{\alpha_w}{\alpha_i} = \text{downwash factor}$$

The origin of the coordinate system lies on the plane of symmetry of the wing in the "bound vortex" which for every α was assumed to be located in the c.p. of the wing on the plan form of the profile.

Figure 6 illustrates the experimentally defined downwash factors for four lateral axes.

Figure 7 gives the experimental values for six normal axes in addition to one normal axis at $\epsilon_l = 1.0$ distance. The formula for it is:

$$\frac{\alpha_w}{\alpha_i} = \frac{\frac{1}{2}\left[\frac{1}{\epsilon_h^2+k^2} + \frac{1}{\sqrt{\epsilon_h^2+k^2+1}}\left(\frac{1}{\epsilon_h^2+k^2} + \frac{1}{\epsilon_h^2+1} \right) \right]}{1 + \frac{c_a}{\pi} \frac{F}{b^2} \frac{\epsilon_h}{\epsilon_h^2+1} \frac{1}{\sqrt{\epsilon_h^2+k^2+1}}} \tag{10}$$

when the theoretical vortex system is exchanged for a trailing vortex with $a = kb$ tip-vortex spacing. The denominator varying so little from 1, the evaluation with the numerator was adequate.

Figure 8, in addition to the downwash factors for six superimposed longitudinal axes, also shows the theoretical curves relative to the ϵ_l axis through the origin of the coordinates for:

a) "Upper limit"

b) "Lower limit"

c) Elliptical lift distribution, vortex sheet rolled up, k = 0.785

d) Rectangular lift distribution, vortex sheet rolled up, k defined on the simple premise of lift gradient $\dfrac{dc_a}{d\alpha_\infty} = 2\pi$ (k = 0.865 for λ = 5)

Figure 9 depicts, other than the already cited theoretical curves for the longitudinal axis, four other theoretical curves (dashes) computed with k values for rectangular lift distribution, according to Betz.

The striking fact of the downwash curves recorded on the lateral axes (fig. 6) is their peculiar wavelike aspect, which seems to be so much more pronounced as the angle of attack is smaller. The waves lie in flow direction, so that curves recorded on longitudinal axes do not exhibit this wavy effect, and curves of successive lateral axes are in parallel direction. The phenomenon may tie in with the fact that the predetermined free jet of the 2.25-meter wind tunnel manifests appreciable changes in flow direction over the cross section.

Leaving aside the waviness of the curves, their general shape may be summed up as follows: Up to about $\epsilon_q = \pm0.6$, a slight rise in angle of downwash of approximately $0.2\,\alpha_i$, that is, about 1° at the highest, is noticeable, in contrast to the practically constant angle of downwash within range of the span of the control surfaces of an airplane, i.e., within range of $\epsilon_q = \pm0.25$; whence it was not deemed necessary to plot a theoretical curve in the graph. Above $\epsilon_q = \pm0.6$, the angle of downwash decreases when the lateral axis is above or below the wing; it rises when the lateral axis intersects the tip vortices.

According to all recorded normal axis diagrams, the normal axis curves (fig. 7) manifest that the pressure-side records are a little higher than the theoretical values, although the shape of the experimentally defined curves is about the same as that of the theoretical curves. Contrariwise, the suction side reveals, with increasing ϵ_h, a more severe drop of the experimental values than the theoretical curve indicates. This may perhaps be explained by the wake flow, which edges itself wedgelike between the air sweeping along above and below the wing and consisting chiefly of slowed-up air particles sweeping along above the wing.

The diagram of the downwash curves for $\alpha = 8.6^\circ$ (fig. 8), recorded on the longitudinal axes, reveals the following: The two curves recorded for $\epsilon_h = -0.0702$ and $\epsilon_h = +0.0298$, are approximately coincident and consequently also with the curve for $\epsilon_h = 0.0$. These curves lie in the approximate center of the "theoretical" curves for $k = 0.785$ (elliptical lift distribution, vortex sheet rolled up) and $k = 0.865$ (rectangular distribution, vortex sheet rolled up), whence they were amenable to predetermination by introducing $k = 0.825$. The percent discrepancy of the experimental from the theoretical values computed with $k = 0.865$, is approximately 10 percent.

The steepness of the experimental curve in model proximity over that arrived at with an assumed trailing vortex, is primarily attributable to the still unfinished rolling process of the vortex sheet in model proximity. The values, as a result, approach the "upper limit." A further reason may lie in the finite wing chord since, as will be remembered, the wing was exchanged for an effective line in the formulation of the equations.

The downwash factors over the longitudinal axes for $\epsilon_h = 0.0$ with increasing α (fig. 9), reveal a certain regularity in curve position. The curves for small α, for which $n = \dfrac{dc_a}{d\alpha} = $ constant, that is, up to about $c_a = 0.9$, are almost coincident. These curves are highest, and approach the theoretical curve for $k = 0.785$ at $\epsilon_l = 0.5$, and drop at $\epsilon_l = 2.0$ between those for $k = 0.785$ and 0.865, in contrast to that for $\alpha = 14^\circ$, which already intersects the theoretical curve at $k = 0.865$. Using the theoretical curves for k values plotted in

the graph, according to Betz's more exact method for comparison, the theoretical curves themselves drop lower as α increases. Thus, the behavior of the curve position is as established by the theory. Even so, the noticeable fact remains that the discrepancy of the experimental curves from the dashed theoretical curves is so much greater than from full-drawn theoretical curves. As k then is proportional to the spacing of the tip vortices, it would be indicative of a tip vortex spacing smaller than the theory predicts.

Yet the measurements of this spacing on the elliptical wing actually prove it to be greater rather than smaller - a fact which stresses the need for further investigations before the theoretical and the experimental downwash formulas can be reconciled.

b) Rectangular wing, airfoil No. 422.- Figure 10 is the polar diagram of airfoil No. 422, taken from Ergebnisse der Aerodynamischen Versuchsanstalt zu Gottingen, volume I.

The angle of downwash was measured on several axes (on two stations) for $\alpha = 4.2^\circ$ and $\alpha = 8.1^\circ$. The results were identical with those for the rectangular wing No. 387.

A comparison of the downwash factors of profile No. 422 with those of No. 387, on the basis of the longitudinal-axis curves in plane of symmetry of the wing at $\epsilon_h = 0.0$, reveals the following: The longitudinal-axis curves recorded at $\alpha = 4.2^\circ$ and 8.1° differ in model proximity at most, only about 0.3°, so that both angles of attack may be expressed by a mean curve which, if plotted in figure 9, would bring it approximately between curves (1) and (2) up to $\epsilon_l = 1.5$ and then, as ϵ_l increases, closer to curve (1). Since the mean value of $n = \dfrac{dc_a}{d\alpha} = 3.45$, corresponding to curve (2), the downwash factors of airfoils Nos. 387 and 422 may be said to agree very well for practical requirements. This statement should undoubtedly hold for all similar profiles.

c) Elliptical wing, airfoil No. 387.- The aerodynamic force measurements are shown in figures 11 and 12.

The downwash measurements again consist of a first and a check test and, in addition, of a record on several longitudinal axes at $\alpha = 8.6^\circ$ with turbulence grid. The

reason for the latter test was that in the test without turbulence grid, the downwash curves on the longitudinal axis varied quite considerably from those of the preceding rectangular wing, which was indicative of a lift distribution not in accord with the desired elliptical distribution. A comparison of the elliptical-wing polar without turbulence grid with the rectangular-wing polar, confirmed this suspicion: that of the elliptical wing was more to the right in the graph. It was presumed that this occurrence was related to low Reynolds Numbers of the outer profiles of the elliptical wing, and that a turbulence grid would modify both polar and angle of downwash. But it was found in the force measurement that the polar with and without turbulence grid differed only as to maximum c_a value; even so, it modified the downwash factors, as shown elsewhere in the report.

The first test was made at $\alpha = -0.2^\circ$, 4.5°, 8.6°, and 14°, the check test at the same angles and, in addition, at $\alpha = -3.2^\circ$. The results are shown in figures 13-17.

The lateral axis measurements revealed nothing basically new, according to figure 13.

In the normal axis measurements (fig. 14), the noncompliance with the theoretical curves is much greater than for the rectangular wing. The only similarity remaining is that here the discrepancies in the field of flow below the pressure side of the wing exceed those on the suction side.

As to the longitudinal axis measurements themselves, the discussion is restricted to the mean measurement of figure 17, where, as it is noted, the first and second tests were almost in perfect agreement,* especially at $\alpha = 8.6^\circ$ and 14°.

Figure 17 manifests a certain relationship with the rectangular wing of figure 9, except for the following:

---

*Both angles, having the same lift gradients, angles $\alpha = -3.2^\circ$ and $\alpha = -0.2^\circ$, were collected in figure 17.

a) At $\alpha = -3°$ to $+14°$, the individual curves are
farther apart; that is, the enclosed angle of
downwash range is greater.

b) The curves are higher in the graph. For both the
rectangular and the elliptical wing, the curve
for maximum α with adhering flow intersects
the theoretical curve (at $k = 0.865$ for the
rectangular wing; at $k = 0.785$ for the ellip-
tical wing). The uppermost curve for the ellip-
tical wing intersects the curve for the "upper
limit" at $\epsilon_l = 1.2$, while that of the rectan-
gular wing falls short of this "upper limit."
The markedly high values in model proximity
may, in part, be attributable to a profile chord
effect, the chord at wing center being equal to
$b/4$.

c) The curves are steeper.

Mention should be made of figure 15, which illustrates
the effect of the turbulence grid, and the probable effect
of a higher Reynolds Number at $\alpha = 8.6°$. At this angle,
the c_a value is a little higher with than without the
grid. The $n = dc_a/d\alpha$ value is smaller. The downwash
curves are, accordingly, lower than for the model without
turbulence grid.

III. EXPLORATION OF POSITION OF TIP-VORTEX CORES

ON ELLIPTICAL WING

1. Test Procedure

The location of the border of the vortex area as meas-
ured on the elliptical wing, is identical with the location
of the cores of the individual tip vortices at greater dis-
tance behind the wing. The edges of the vortex area or
vortex cores are readily observed on streamers which exe-
cute rapid conical rotary motion. Admittedly, this rotary
motion of the streamers is not confined to a point, but
rather extends over a circular section of about 1 to 3 cm
(0.3937 to 1.18 in.) diameter, depending on the amount of
angle of attack. The location of the borders is defined
by the center of the circle. The results for three angles
of attack are given in figures 18 and 19. The spacing of

the tip vortices in figure 18 shows the asymptotic approach
of these tip vortices, according to the theoretically pre-
scribed spacing $b' = kb$. The distance is a little less
as α is higher, although the discrepancies are minute.
The concentration of the span-distributed vortices in two
separate tip vortices, terminates, according to a British
report (reference 5), at around $\epsilon_l = 4$ where, of course,
the theoretical spacing $b' = 0.785\ b$ of the vortices,
has not as yet been reached, according to figure 18. On
the contrary, it amounts to around $0.85\ b$ in the range of
$\epsilon_l = 2$ to 4. In accord with that, the downwash factors
must be less than given in the theoretical curves of the
graphs showing the downwash factors plotted against ϵ_l (at
$\epsilon_h = 0$). Plotting the theoretical curve of α_w/α_i for
$k = 0.85$ in figure 17, which lies by about $\alpha_w/\alpha_i = 0.25$
lower than the dashed curve for $k = 0.875$, would reveal,
on the other hand, that curve (4) for $\alpha = 14^0$ itself lies
higher than the theoretical curve for $k = 0.85$.

Examination of the difference in height of the tip
vortices from the longitudinal axis of the chosen coordi-
nate system (fig. 19), reveals the following: The curves
of the tip vortices start exactly in the pressure line of
the wing which, owing to its flat pressure side, lies at
the wing tips in the wing chord. The curve is, at first,
parabolical, then deflects at $\epsilon_l = 1$ to 2, and finally
becomes straight lines, parallel to the longitudinal axis.
The distance of this parallel line from the longitudinal
axis is, at the most, approximately equal to the chord in
wing center - that is, insignificant, so that in this re-
spect the assumptions of trailing vortex in flow direction
for computing the downwash factors, are satisfactorily
complied with.

2. Comparison of Recorded Position of the Tip-Vortex Cores
with the Kaden-Betz Theory (reference 1)

In his thesis "Development of an Unstable Area of Dis-
continuity," Kaden employs terms for the position of the
spiral center of an area of discontinuity which, as is
known, coils up in the form of a spiral. This area of dis-
continuity moving vertically downward at constant velocity,
is thereby bounded on one side only. But, when assuming
the rolling-up process at the edges to be the same for a
sufficiently wide vortex sheet, the latter may be visual-
ized as being produced by a wing with elliptical lift dis-

tribution. The center of the helix with the tip-vortex
cores, described in the preceding section, can also be ap-
proximately identified because - as Kaden himself showed -
at greater distance behind the wing the circulation about
the center of the spiral is such as if only one concen-
trated vortex existed. Besides, the premise for the start
of the rolling process is that the circulation about the
spiral center is the same as around a vortex filament -
when the circle around the spiral center for which the
circulation is computed, is not too small. On these prem-
ises, the results of the preceding section can be compared
with Kaden's theoretical findings.

Then the term for the diminished spacing of the tip
vortices reads:

$$\frac{a}{b/2} = 0.68 \left(\frac{c}{b}\right)^{2/3} \tag{1}$$

and that for the rise of the tip vortices over the lowest
point of the vortex sheet:

$$\frac{h}{b/2} = 1.04 \left(\frac{c}{b}\right)^{2/3} \tag{2}$$

Hereby $a = \frac{b - b'}{2}$ and $c = w\,t$ is the displacement of
the area of discontinuity, when w = vertical velocity of
said area, and t = time interval.

Disregarding the rolling-up process, the vertical ve-
locity of the area of discontinuity of a wing with ellip-
tical lift distribution is, at great distance behind the
wing, equal to twice the interference velocity at the
point of the wing:

$$w = 2w_0 = 2\,\frac{c_a}{\pi}\,\frac{F}{b^2}\,V_0$$

This value must be written in (1) and (2) because the pre-
scribed circulation distribution in the vortex area is
directly tied to this quantity; that is, this value is a
measure for the intensity of the vortex area.

In order to be able to compare the theoretical curve
of the rise $\frac{h}{b/2}$ of the tip vortices to be computed with
these values, against the experimental values of the posi-
tion of the tip vortices, we establish the apex of the

vortex area in the plane of symmetry of the wing, as h can be approximated from this lowest point of the vortex area. Strictly speaking, this holds true only so long as the rise h is very small compared to the width of the vortex sheet. This point can be established by recording the wake vortex area with a total-head survey apparatus. The position of the minimum of the total head is identical with the point under consideration. The measurement was made - for other reasons -.for two spacings behind the wing. Another way would be to define the position by means of the recorded downwash factors on the longitudinal axis passing through the wing trailing edge, through integration of these factors over ϵ_l. With $\dfrac{\alpha_w}{\alpha_i} = z$ and $w =$ interference velocity at point ϵ_l, we have:

$$\alpha_w = \frac{w}{V_0} \; ; \; w = \alpha_w V_0 = z \, \alpha_i \, V_0$$

$$c = \int_0^{\epsilon_l} w \; d \; t; \; t = \epsilon_l \, \frac{b/2}{V_0} \; (\text{since} \quad l = V_0 \; t)$$

$$\epsilon_c = \frac{c}{b/2} = \alpha_i \int_0^{\epsilon_l} z \; d \; \epsilon_l$$

Figure 19 (curve 1) shows the ϵ_c values for $c_a = 1.07$ as obtained by graphical integration of the z values for $\epsilon_h = -0.09$ in figure 15. The start of the integration was at $\epsilon_l = 0.32$, the figure for the trailing edge of the profile. The corrections for the finite jet diameter afforded curve (2) of figure 19.

It is seen that the ϵ_c value of the wake-flow measurement is in very close agreement with the thus-computed ϵ_c values. The minor discrepancy at $\epsilon_l = 2.33$ is attributable to the fact that at greater distances the z values should really have been taken on a longitudinal axis with $\epsilon_h = -0.4$. For the rest, the close accord is indicative of the practical usefulness of the employed method of recording the angle of downwash. Lastly, we extrapolated the thus-established curve in the $\epsilon_l = 0$ to 0.5 range to the point of the effective line in the wing chord, so as to more closely approach the conditions existing at the wing tips (curve 3).

Then curve (4), computed according to the Kaden-
Betz theory, is in very exact agreement with the measured
curve as far as $\epsilon_l = 2.0$, where the curve then gradually
turns parallel with the longitudinal axis. Perhaps the
assumption that the rolling-up process ends in this point,
is legitimate.

Kaden cites a different point for the termination of
the spiral process. He proceeds from the assumption that
the speed of rolling up, i.e., the rate at which the edges
of the vortex sheet approach the wing center - that is,
the quantity

$$u = \frac{da}{dt}$$

preserves its initial value until the distance

$$a_{max} = \frac{b - b'}{2}$$

has been covered.

Curve (1) in figure 18 illustrates the values of the
position of the tip vortices for $c_a = 1.07$ as computed
from $\frac{a}{b/2} = 0.68 \left(\frac{c}{b}\right)^{2/3}$. This theoretical curve agrees on-
ly in wing proximity to some extent with the experimental-
ly defined values. At constant rolling-up speed, the path
of the tip vortices would be represented by a tangent in
the origin of the theoretical curve (1). The intersection
of the tangent with the line parallel to the axis of the
abscissa, which denotes the theoretical end position of the
tip vortices, would then give the point at which the roll-
ing-up process terminates. It lies, according to Kaden, at
$\epsilon_l = 0.568 \cdot \frac{b^2}{F} \cdot \frac{1}{c_a}^{*}$, that is, at $\epsilon_l = 2.65$ for $c_a = 1.07$.

The agreement with $\epsilon_l = 2.0$ taken from figure 19,
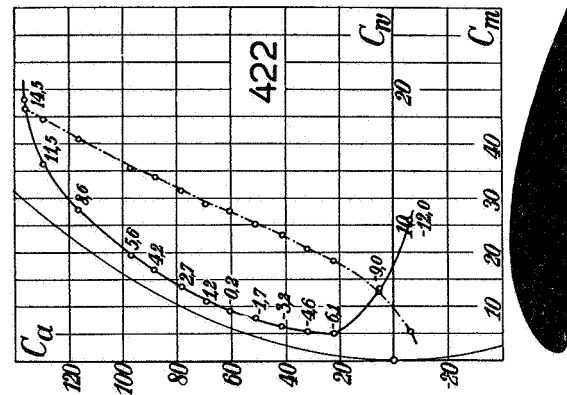is therefore, close.

------

*Allowing for a factor 3.2, for which Kaden's figures are
erroneously given too low.

Translation by J. Vanier,
National Advisory Committee
for Aeronautics.

REFERENCES

1. Kaden, H.: Aufwicklung einer unstabilen Unstetigkeits-
      flache. (Diss. Gottingen, 1931.) Ing.-Archiv Jg.
      2 (1931).

2. Prandtl, L.: Theory of Lifting Surfaces. Part II.
      T.N. No. 10, N.A.C.A., 1920.

3. Helmbold, H. B.: Über die Berechnung des Abwindes hin-
      ter einem rechteckigen Tragflügel. Z.F.M., Bd. 16,
      No. 15, p. 291.

4. Betz, A.: Behavior of Vortex Systems. T.M. 713,
      N.A.C.A., 1933.

5. Fage, A., and Simmons, L. F. G.: An Investigation of
      the Air-Flow Pattern in the Wake of an Aerofoil of
      Finite Span. Phil. Trans., Roy. Aero. Soc. of London,
      series A, vol. 225; also R. & M. No. 951, British
      A.R.C., 1925.

6. Glauert, H.: The Elements of Aerofoil and Airscrew
      Theory, chap. XII, 1926. The University Press, Cam-
      bridge, England.

7. Betz, A.: Contribution to Airfoil Theory with Special
      Reference to the Simple Rectangular Wing. Diss.,
      Gottingen, 1919.

8. Kroner. Z.V.D.I., Bd. 61 (1917), No. 29, p. 606.

9. Christiani, K.: Experimentelle Untersuchung eines Trag-
      flugelprofils bei Gitteranordnung. Luftfahrtforschung,
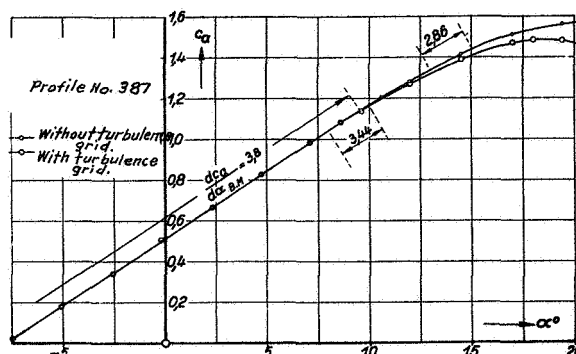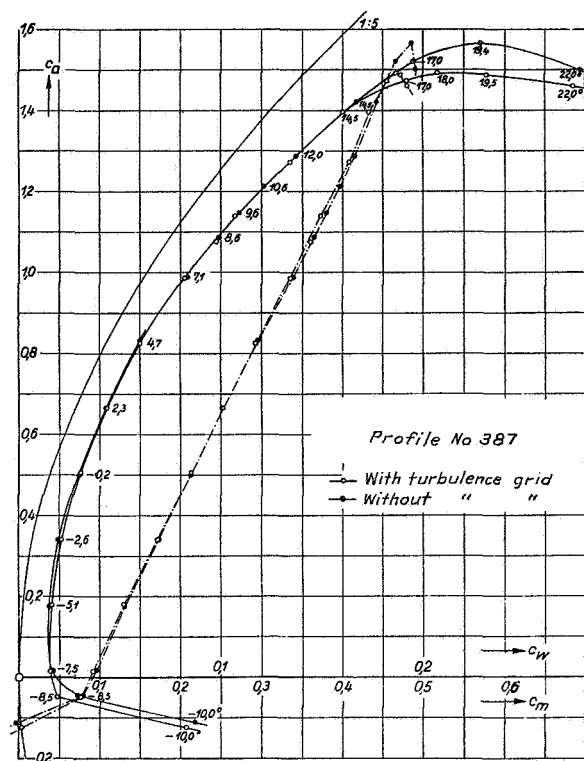   Bd. 2, No. 4, p. 101.

Figure 1.- Distribution of
vortices behind
the wing.

Figure 2.- Theoretical downwash factors
for different tip vortex
spacing.

Figure 3.- Tip-vortex spacing on
rectangular wings.

Figure 4.- Polar of rectangular
airfoil No. 387. 1:5

Figure 5.- Rectangular wing; downwash
factor versus angle α.

Figure 6.- Rectangular wing; downwash factors for
four transverse (lateral) axes.

Figure 10.— Polar diagram for airfoil No. 422

Figure 9.— Rectangular wing; theoretical and experimental downwash factors for the longitudinal axis through the origin of the coordinates at various angles α.

Figure 7.— Rectangular wing; downwash factors for six vertical axes in plane of symmetry of the wing.

Figure 8.— Rectangular wing; downwash factors for six longitudinal axes in plane of symmetry of wing.

21

Profile No 387

—○— With turbulence grid
—•— Without   "   "

Figure 12.- Elliptical wing;
c_a versus α .

Figure 11.- Polar of elliptical
wing 1:5;
airfoil No. 387

Elliptical wing   1:5, Profile No 387
$\alpha=8,6°$, $c_a=1,07$, $\alpha_i=3,90°$
—○— $\varepsilon_h=0,1106$, $\varepsilon_l=1,344$
—•— $\varepsilon_h=-0,0895$, $\varepsilon_l=1,344$
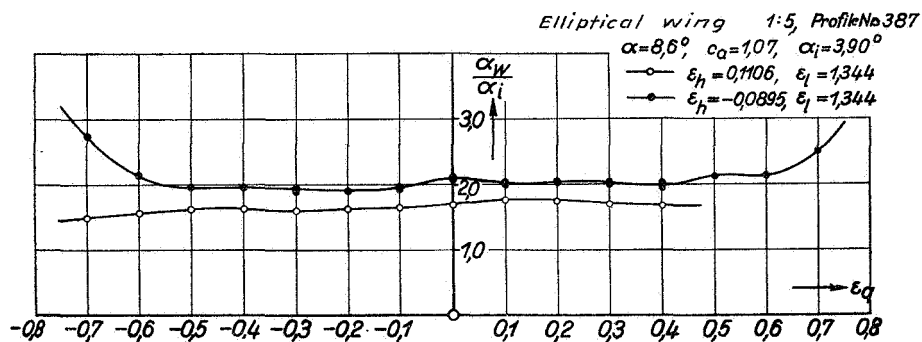
Figure 13.-
Elliptical
wing; down-
wash factors
for two
lateral axes.

Elliptical wing   1:5, Profile No 387
$\overline{\alpha}=8,6°$, $c_a=1,07$, $\alpha_i=3,90°$
$\varepsilon_q=0,0$
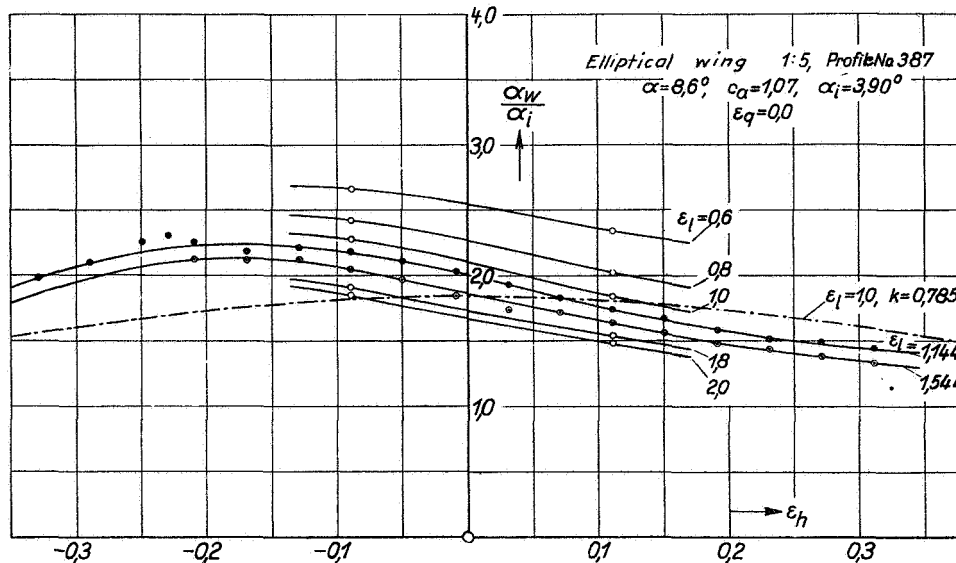
Figure 14.-
Elliptical
wing;
downwash
factors
for six
vertical
axes in
plane of
symmetry
of wing.

22
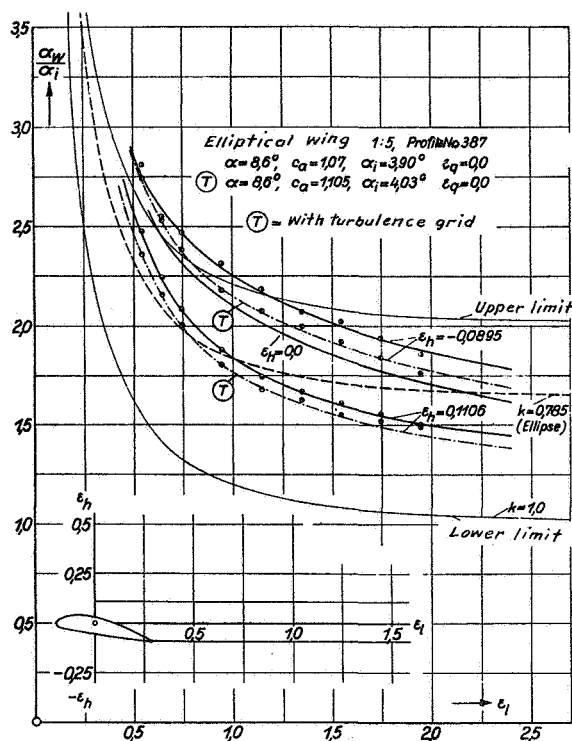
Figure 15.-
Elliptical wing;
downwash factor
for two longitu-
dinal axes in
plane of
symmetry of
wing, measured
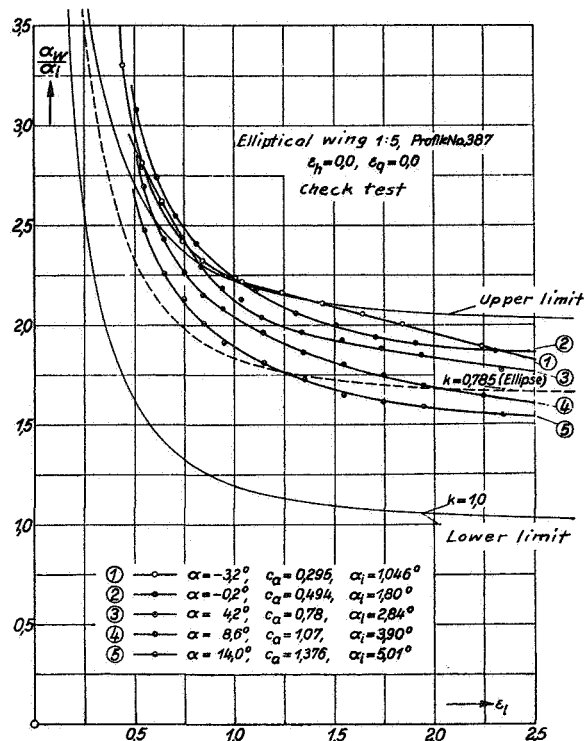with and without
turbulence grid.

Figure 16.-
Elliptical wing;
downwash factors
for the longitu-
dinal axes
through the
origin of the
coordinates for
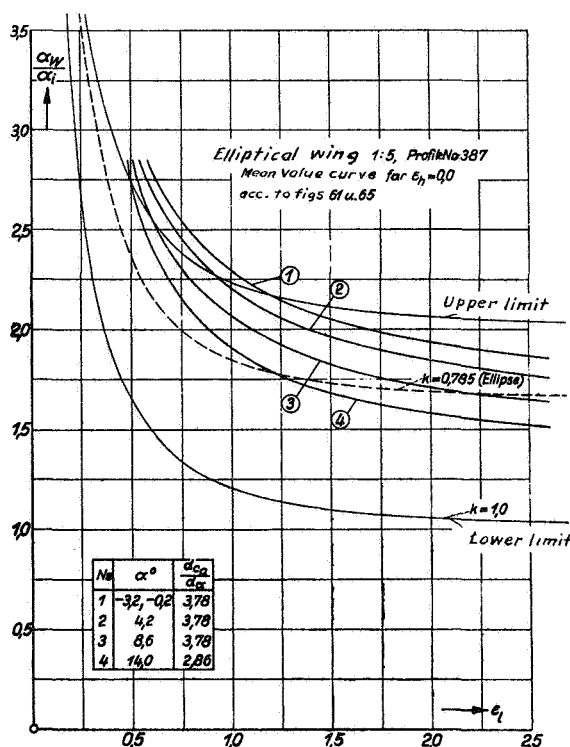different α
(check test).

Figure 17.- Elliptical wing; downwash factors for
the longitudinal axes through the
origin of the coordinates for different α
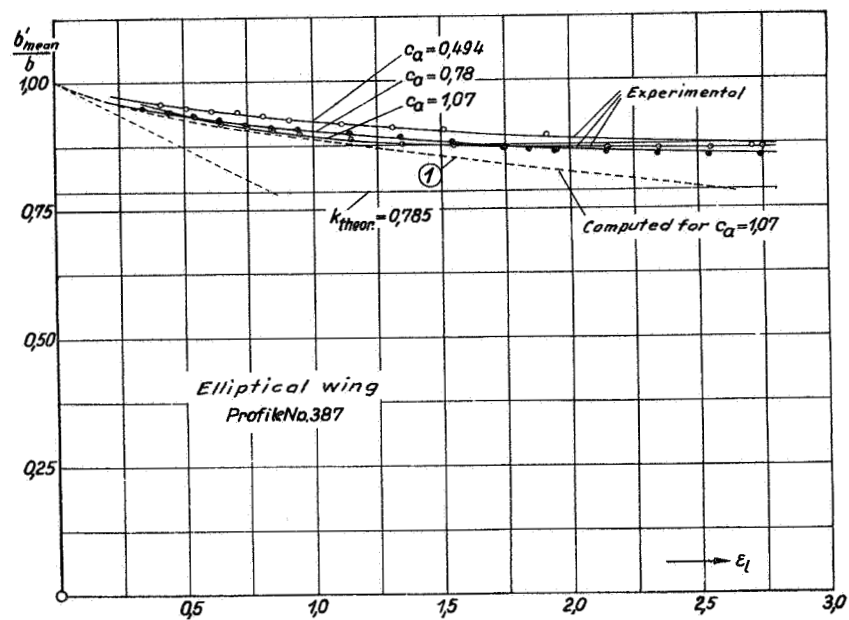(mean values).
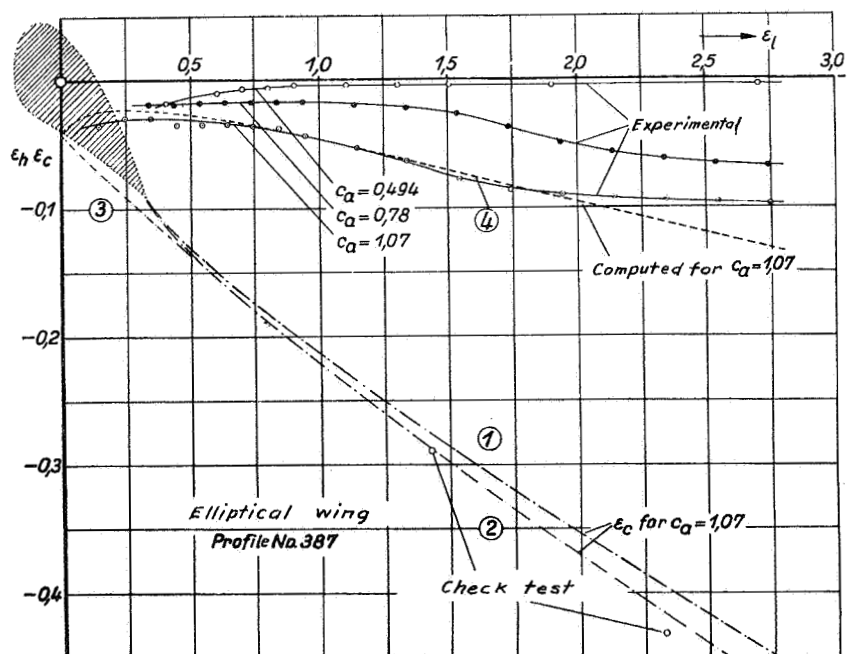
23

Figure 18.- Distance of tip vortices on elliptical wing.

Figure 19.- Height of tip vortices on elliptical wing.